Proceedings of the EuroGNC 2013, 2nd CEAS Specialist Conference
on Guidance, Navigation & Control, Delft University of Technology,
Delft, The Netherlands, April 10-12, 2013

Nonlinear Non-Cascaded Reference Model Architecture for Flight Control Design with Flight Path Angle Rate Command System

Fubiao Zhang, Florian Holzapfel, Matthias Heller

Abstract A nonlinear reference model architecture motivated by dynamic inversion based flight control is introduced. As a novel feature, only one integrated reference model is used to provide reference commands, for longitudinal axis: the flight path angle, vertical load factor (or angle of attack) and pitch rate, while admitting flight path rate command as input; for lateral axis, bank angle and roll rate; for directional axis, lateral load factor and yaw rate. Flight dynamics, actuator dynamics with rate and position limits, and envelope protections can also be incorporated in a straight forward way in one reference model. One advantage of this non-cascaded reference model is that at least the attitude of the reference response can be restored and flied at an early stage of the flight control system design cycle. The second feature is that the reference model is parameterized, allowing the opportunity of updating the knowledge of aircraft dynamics (e.g. damaged) and flying qualities design. With these two aspects, the physical consistency in terms of the reference commands among different channels and reference commands reasonable with respect to true aircraft dynamics can be assured. Although designed for General Aviation aircraft, the framework can be generalized for other aircrafts considering only rigid body dynamics.

Nomenclature

A	Aerodynamic frame
B	Body-fixed frame
O	NED frame
E	Earth centered earth fixed frame
K	Kinematic frame

Fubiao Zhang·Florian Holzapfel·Matthias Heller, Institute of Flight System Dynamics (FSD), Technische Universität München (TUM), D-85748 Garching, Germany
e-mail: fubiao.zhang@tum.de, florian.holzapfel@tum.de, matthias.heller@tum.de

2

$\overline{K}$	Rotated kinematic frame
L, M, N	The moments around x, y and z axis of B frame, respectively
p, q, r	Angular rates around x, y and z axis of B frame, respectively
θ, ϕ, φ	Pitch angle, bank angle, azimuth angle, respectively
γ_K, μ_K, χ_K	Flight path angle, flight path bank angle, flight path azimuth angle, respectively
α, β	Angle of attack, sideslip angle, respectively
η, ξ, ζ	Elevator, aileron and rudder deflection, respectively
V_A^G	Aerodynamic speed of the Center of gravity
V_K^G	Kinematic speed of the Center of gravity
$\dot{\rho}_{\overline{K}}$	Modified flight path angle rate, $\dot{\rho}_{\overline{K}} = \dot{\gamma}_K / \cos \mu_K$
$\overline{q}$	Dynamic pressure
c	Command signal
ff	Feed forward signal
r	Reference signal
$extra$	Extra command compared to signal limit
alw	Allowed magnitude of the signal

1. Introduction and Motivation

Fly-by-Wire control systems have been successfully applied in both commercial and military aviation for several decades, despite its high price and complexity, this paper presents part of the efforts to apply this concept in the General Aviation aircraft, in an attempt to make flight safer and more intuitive.

Many general aviation aircrafts are operated by only one pilot, with envelope protection and high automation, fly-by-wire control systems can offer carefree handling, relieving the pilot from tedious stabilizing work. The more pilot is unburdened from a low-level, high frequency routine handling tasks, the more attention he can pay for other higher level tasks, e.g. navigation, communication, making decisions in case of adverse weather condition and so on. It might be safe to say one basic higher level task of manual flight control is to change the flight path, to this point, flight path angle rate command seems reasonable, as it gives pilot direct influence on a state at a higher end of the control loops, while the inner loop (i.e. pitch attitude, pitch rate) control tasks can be automatically executed by the flight control laws, thus the workload could be reduced while equal or better performance could be expected. From a handling qualities point of view, it also makes sense to interpret the pilot's stick (command) inputs as flight path rate. Because within the pilot's operation bandwidth, it is highly desirable to achieve a $1/s$

structure from pilot's input to the targeted variable to be controlled, which is generally speaking the flight path.

Pioneer work has been done focusing on flight path augmentation [1-4], encouraging the command system in this paper. For instance in Ref [1], a flight path angle and ground track control wheel steering system was proposed to reduce pilot's workload and improve safety during maneuvering. In Ref [2], the author described the 7J7 manual control functions, which was also featured by flight path rate command, and concluded that the functions are favorably received by pilots from major airlines in the simulator tests. As for general aviation aircraft [3], piloted simulation results also showed that direct influence on flight path got positive feedback from the pilots. The authors of Ref [4] compared three different command systems with conventional Fokker 100: a rate command system, a flight path vector command system and a C^* command system, the results are that the fly-by-wire control system itself does not improve performance significantly, however, when equipped with a flight director system, the flight path command system reduced much workload. Recent research conducted in TU Delft investigated the integration of flight path oriented control and perspective flight path displays [5-6].

The paper at hand is limited to the flight path control problems only without dealing with display designs. Here a modified flight path angle rate command $\dot{\rho}_{\overline{K}}$ in the rotated kinematic frame ($\overline{K}$) is proposed, that is for flight in the vertical plane, pilot's stick deflection is seen as flight path angle rate command $\dot{\gamma}_K$ in the kinematic (K) frame, however, when the aircraft banked from the flight path, the stick deflection is interpreted as commanding a change in the flight path rate in the vertical symmetric plane. A comment to be made here is that the actual feedback variable does not have to be the same as command, here γ_K could be used to stabilize the inertial flight path angle.

To implement a $\dot{\rho}_{\overline{K}}$ command system, this paper presents a novel reference model architecture. This architecture was motivated by building only one integrated, physically meaningful, non-cascaded reference model to provide reference commands of different channels in the dynamic inversion based flight control. By contrast, many of the popular designs use cascaded reference models. The advantages could be explained later. However, the application of this concept is not restricted to dynamic inversion based control applications, other model following based design can also utilize its advantages.

2. Functionality Requirements of the Flight Control System

The reference model design is driven by the functionality requirements of the flight control system. Requirements documents were formulated quite detailed before the flight control design started. These functionality requirements shall be met

in terms of desired performance or less restrictive adequate performance when the control loop is closed. Since the reference model design itself is forming ideal dynamic behavior of the closed system, it is actually open loop specifications, without considering temporarily the influence of the error dynamics introduced by feedback. The error dynamics, on the other hand, would deteriorate the ideal performances when there is disturbance or uncertainty in the plant model. With this in mind, the desired performance must be met by the reference model itself. As far as this paper is concerned, several desired performance requirements are listed.

Table 1. High Level Functionality Requirements

No.	Functionality	Desired Performance
1	Flight path angle rate command	$\delta F_{s,lon} = \dot{\rho}_{\bar{K}}$
2	Flight path angle Limitation	$-25^\circ \le \gamma_K \le 25^\circ$
3	Pitch angle limitation	$-50^\circ \le \theta \le 50^\circ$
4	Load factor limitation	$-1 \le (n_z)_B \le 3.8$
5	AoA protection	$-5^\circ \le \alpha_A \le 12^\circ$
6	High(low) speed limitation	$V_s \le V_A \le V_{\max}$
7	Turn compensation	$\Delta n_{z,c} = \Delta n_{z,turn\_compensation}$
8	Turn coordination	$\dot{\theta} = 0, \dot{\phi} = 0, (n_y)_B = 0$
9	Velocity vector roll	$r_K / p_K = \tan\alpha_A$
10	Bank angle limitation	$-75^\circ \le \phi \le 75^\circ$
11	Spiral stability	Neutral stable: $-48^\circ \le \phi \le 48^\circ$ Stable: $48^\circ \prec \lvert\phi\rvert \le 75^\circ$
12	Trimmed AoA limitation	$-2^\circ \le \alpha_{trim} \le 9^\circ$

3. Transition of Functionality Requirements to Design Constrains

In this section, functionality requirements are interpreted in a lower operational level to guide the flight control design.

3.1. Modified Flight Path Angle Rate Command

For flight path angle rate command realization, here a new variable $\dot{\rho}_{\bar{K}}$, modified flight path rate, is introduced. As mentioned above, $\dot{\rho}_{\bar{K}}$ is equivalent to $\dot{\gamma}_K$ for non-turn maneuver, whereas for turning flight $\dot{\rho}_{\bar{K}}$ corresponds to the rotation rate of velocity vector in the symmetric plane. The force situation is illustrated in Figure 1 (a) in the rotated kinematic frame ($\bar{K}$), when the external force in the z-axis of $\bar{K}$ frame is tilted. Two equations could be concluded to illustrate what $\dot{\rho}_{\bar{K}}$ means:

$$\Delta(n_z)_{\bar{K}} \cdot g = V_K \cdot \dot{\rho}_{\bar{K}} \tag{1}$$

$$\dot{\rho}_{\bar{K}} = \dot{\gamma}_K / \cos\mu_K \tag{2}$$

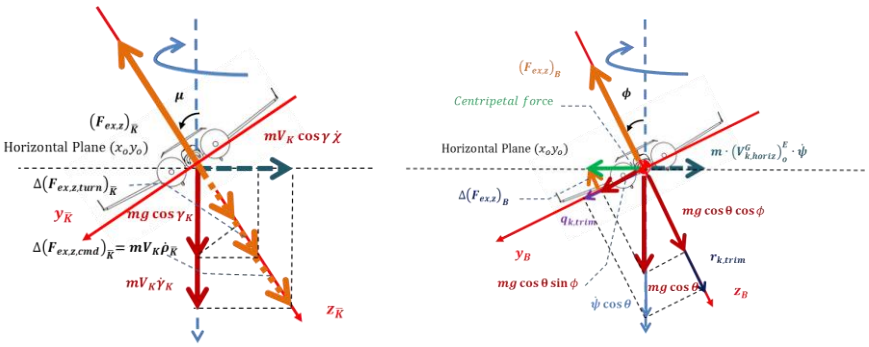

(a) (b)

Fig. 1. Turn Analysis in $\bar{K}$ (a) and B (b) Frame

3.2. Turn Compensation

A natural choice for considering turn compensation in the flight path dynamics environment would be in the $\bar{K}$ frame, as shown in figure 1(a). External force (excludes gravity) along the rotated kinematic frame z-axis $(F_{ex,z})_{\bar{K}}$, which mainly comes from lift, contributes in two aspects. First, $(F_{ex,z})_{\bar{K}}$ balances the gravity component on the z-axis, which is $mg\cos\gamma_K\cos\mu_K$. On the other hand, one part of $(F_{ex,z})_{\bar{K}}$ is used for turn compensation, here called $\Delta(F_{ex,z,turn})_{\bar{K}}$. The turn com-

pensation part acts together with the gravity component on $\overline{K}$ frame y-axis, which is $mg\cos\gamma_K \sin\mu_K$, to provide the necessary centripetal force for the turn. Or put it in another way,

$$\left(F_{ex,z}\right)_{\overline{K}} = \underbrace{mg\cos\gamma_K\cos\mu_K}_{gravity\_balancing} + \underbrace{\Delta\left(F_{ex,z,turn}\right)_{\overline{K}}}_{turn\_compensation} = mg\frac{\cos\gamma_K}{\cos\mu_K} \tag{3}$$

However, μ_K is not directly accessible for measurement and must be calculated from the available sensor signals. In this case, a better analysis might be done in the body fixed frame, as illustrated in figure 1 (b). Then the required external force is

$$\left(F_{ex,z}\right)_B = \underbrace{mg\cos\theta\cos\phi}_{gravity\_balancing} + \underbrace{\Delta\left(F_{ex,z,turn}\right)_B}_{turn\_compensation} = mg\frac{\cos\theta}{\cos\phi} \tag{4}$$

As it is quite desirable that the additionally needed lift could be generated without an intentional command from the pilot, it could be provided automatically by the flight control system, leaving the pilot with less. In this paper, such signals are denoted by the subscript 'trim'. Now the necessary load factor for the compensation is given by:

$$\left(n_{z,trim}\right)_B = \frac{\cos\theta}{\cos\phi} \tag{5}$$

3.3. Constraints for Coordinated Turn

Consider first the attitude propagation equation:

$$\dot{\phi} = p_K + q_K\sin\phi\tan\theta + r_K\cos\phi\tan\theta \tag{6}$$

$$\dot{\theta} = q_K\cos\phi - r_K\sin\phi \tag{7}$$

$$\dot{\psi} = q_K\sin\phi/\cos\theta + r_K\cos\phi/\cos\theta \tag{8}$$

The strapdown equation could be obtained by solving for the rotation rates.

$$\begin{bmatrix} \left(p_K\right)_B^{OB} \\ \left(q_K\right)_B^{OB} \\ \left(r_K\right)_B^{OB} \end{bmatrix} = \begin{bmatrix} 1 & 0 & -\sin\theta \\ 0 & \cos\phi & \sin\phi\cos\theta \\ 0 & -\sin\phi & \cos\phi\cos\theta \end{bmatrix} \begin{bmatrix} \dot{\phi} \\ \dot{\theta} \\ \dot{\psi} \end{bmatrix} \tag{9}$$

Recall the equation of motion of lateral acceleration in the body fixed frame

$$\left(\dot{v}_K\right)_B^{EB} = -\left(r_K\right)_B^{OB}\cdot\left(u_K\right)_B^E + \left(p_K\right)_B^{OB}\cdot\left(w_K\right)_B^E + g\sin\phi\cos\theta + \left(F_y\right)_B/m \tag{10}$$

In a steady state coordinated turn, the following conditions hold:

$$\left(\dot{v}_K\right)_B^{EB} = 0\,,\left(F_y\right)_B = 0 \tag{11}$$

Together with the constraints

$$\dot{\theta} = 0, \dot{\phi} = 0, \left(n_y\right)_B = 0 \tag{12}$$

The rate change of azimuth angle could be solved:

$$\dot{\psi} = \frac{g \sin\phi \cos\theta}{\cos\phi \cos\theta \cdot (u_K)_B^E + \sin\theta \cdot (w_K)_B^E} \tag{13}$$

In the case $(u_K)_B^E$ and $(w_K)_B^E$ from navigation system are not available. An approximation has to be used,

$$\dot{\psi} = g \tan\phi / V_A \tag{14}$$

Until now, to execute the coordinate turn, the following body rotation rates must be generated by flight control system.

$$(p_K)_{B,trim}^{OB} = -\sin\theta \cdot \tan\phi \cdot g / V_A \tag{15}$$

$$(q_K)_{B,trim}^{OB} = \sin\phi \cos\theta \cdot \tan\phi \cdot g / V_A \tag{16}$$

$$(r_K)_{B,trim}^{OB} = \sin\phi \cos\theta \cdot g / V_A \tag{17}$$

3.4. Precondition for Envelope Protections and Phase Plane Based Protection Concept

One precondition for envelope protections is the assurance of the controllability over the aircraft. This is especially true when the dynamic pressure is already quite low. Thus the decrease of the airspeed must not be so fast that no time is left before the aircraft can be recovered from a dangerous situation when the aircraft is actually close to the envelope boundary. Similarly, the increase of the airspeed shall also be limited to avoid overstressing the aircraft.

Here only the high speed limitation requirement is explained, but it illustrates the basis idea of phase plane based protection and merging of other sources of limiting factors. Realization of other requirements are done along with the introduction of the reference model

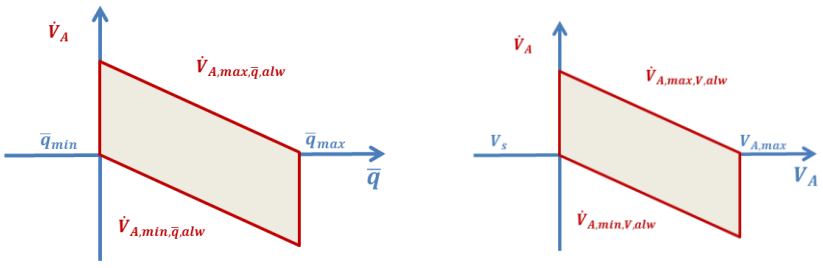

(a) (b)

Fig. 2. Allowable $\dot{V}_A$ in the Grey Area

To prevent the dynamic pressure from going beyond the safe range, the allowed $\dot{V}_A$ is proportional to its distance to the boundary values, as shown in figure 2 (a).

$$\dot{V}_{A,\max,\bar{q},alw} = K_{V_{\max},\bar{q},prot}(\bar{q}_{\max} - \bar{q}) \tag{18}$$

$$\dot{V}_{A,\min,\bar{q},alw} = K_{V_{\min},\bar{q},prot}(\bar{q} - \bar{q}_{\min}) \tag{19}$$

Similarly, $\dot{V}_A$ shall also be limited when the airspeed is close to the boundaries, as shown in figure 2 (b):

$$\dot{V}_{A,\max,V,alw} = K_{V_{\max},V,prot}(V_{\max} - V_A) \tag{20}$$

$$\dot{V}_{A,\min,V,alw} = K_{V_{\min},V,prot}(V_A - V_s) \tag{21}$$

When consider more than one factors, conservative limits should be taken,

$$\dot{V}_{A,\max,alw} = \min\left\{\dot{V}_{A,\max,\bar{q},alw}, \dot{V}_{A,\max,V,alw}\right\} \tag{22}$$

$$\dot{V}_{A,\min,alw} = \max\left\{\dot{V}_{A,\min,\bar{q},alw}, \dot{V}_{A,\min,V,alw}\right\} \tag{23}$$

4. Nonlinear Reference Model Architecture

The reference model is nonlinear in a way that reference commands are formulated by the summation of two parts: trim term and the maneuver part. The maneuver part is the output of the desired linear dynamics. The trim term remains when pilot's stick centered to realize a certain function like turn compensation. Another three common features could be seen later in the reference model: 1) all the output signals are limited by its own upper and lower bound based on physical knowledge. 2) all the inputs of the integrators are limited for the sake of anti-windup. 3) all the reference signals are forward propagated based on the flight dynamics, whereas the saturation (when a certain signal hits the envelope boundary) and boundary overshoot information are backward propagated to the previous integrators to avoid overloading, which is also based on flight dynamics.

4.1. Longitudinal Reference Model

The overall architecture for longitudinal reference model is shown in figure 3.
With

$K_{s,lon}$ Stick scaling gain

$K_{c,lon}$ Dynamic Gain

$M_{actuator}$ Actuator dynamic model with rate and position limits

$M_{aircraft,sp}$ Desired aircraft short period dynamics

M_{load_factor} Algebraic Model of load factor output

M_{path} Dynamic model to generate flight path reference command

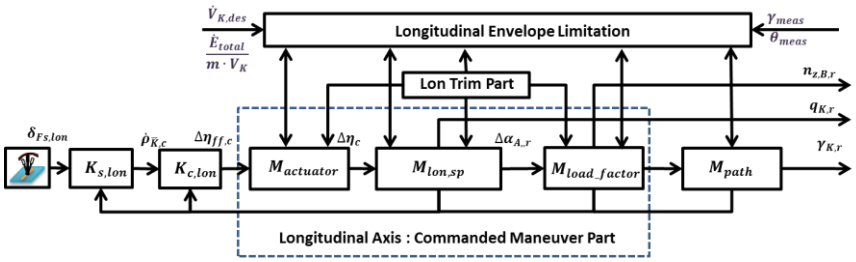

Fig. 3. Architecture of the Longitudinal Reference Model with Limitation

4.1.1. Stick Scaling and Dynamic Gain

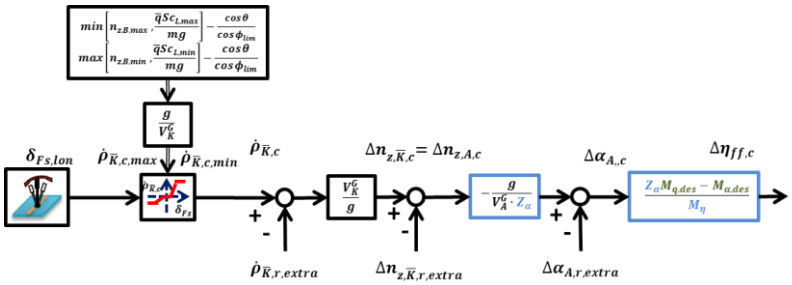

Fig. 4. Stick Scaling and Dynamic Gain $K_{c,lon}$

Figure 4 illustrates how the signal propagates in the feed forward path. The stick scaling gain makes sure the full deflection always commands the largest possible load factor despite changes of flight condition, which is in low speed mainly limited by the aerodynamic capability and high speed the structural stiffness.
With

$$K_{c,lon} = -\frac{V_K^G}{g} \cdot \frac{g}{V_A^G \cdot Z_\alpha} \cdot \frac{Z_\alpha M_{q,des} - M_{\alpha,des}}{M_\eta} \tag{24}$$

The scaled stick command is converted to the commanded input of the elevator model.

4.1.2. Actuator Model with Limits

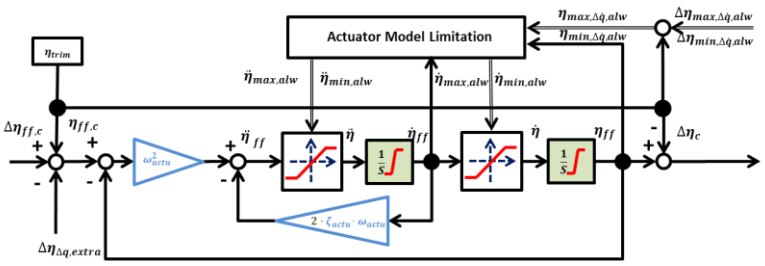

Fig. 5. Actuator Model with Limits

In figure 5, a second order actuator model with acceleration limits, rate limits and position limits is shown here. Therefore the output of the reference model would not be too aggressive to be executed. Besides the limits mentioned above, the back propagated saturation and overshoot information is also taken account on the actuator level.

4.1.3. Desired Short Period Dynamics

The linearized short period dynamics is used here, the subscript "des" indicates they could be specified to reach the desired dynamics. $M_{\alpha,des}$ and $M_{q,des}$ can be designed according to flying qualities requirements (mainly from military standards [12-14]).

$$\begin{bmatrix}\Delta\dot{\alpha}_A\\ \Delta\dot{q}_K\end{bmatrix}=\begin{bmatrix}Z_\alpha & 1\\ M_{\alpha,des} & M_{q,des}\end{bmatrix}\begin{bmatrix}\Delta\alpha_A\\ \Delta q_K\end{bmatrix}+\begin{bmatrix}Z_\eta\\ M_\eta\end{bmatrix}\Delta\eta \qquad (25)$$

This linear dynamics seems to make sense because when the pilot commands a maneuver from a certain trimmed flight, the response of the aircraft is quite predictable. In figure 6, the overshoot information, that excessive command of pitch rate $\Delta p_{K,r,extra}$ is propagated back with a gain $M_{\alpha,des}/M_\eta$, which would convert $\Delta p_{K,r,extra}$ to $\Delta\eta_{\Delta q,extra}$, and subtracted from the actuator command shown in figure 5. In this way, output signals are not hard limited.

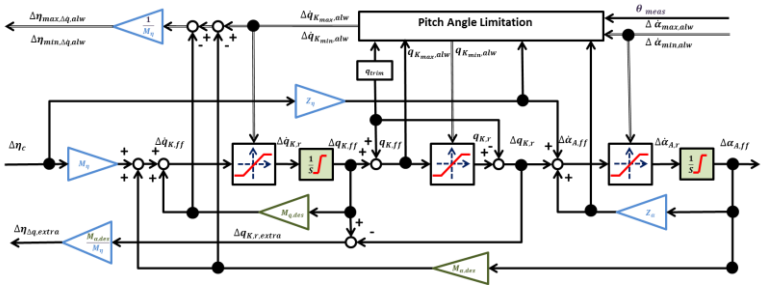

Fig. 6. Desired Short Period Dynamics

4.1.4. Model of Load Factor and Flight Path Angle Reference Command

The maneuver part of the vertical load factor is converted from the AoA with

$$\Delta n_{z,\bar{K},ff} = -\frac{V_K^G \cdot Z_\alpha}{g} \cdot \Delta\alpha_{A,r} \tag{26}$$

Further after limitation is done, inertial flight path rate could be calculated as:

$$\dot{\gamma}_{K,ff} = -\frac{g}{V_K^G} \cdot \cos\phi_{\lim} \cdot \Delta n_{z,\bar{K},r} \tag{27}$$

To be accurate, flight path bank angle μ_K instead of Euler angle $\phi_{\lim}$ should be used. Unfortunately, this is not practical due to measurement problem. However the consequence of this replacement must be evaluated. Figure 7 also showed the back propagation of overshoot information to the dynamic gain part in figure 4.

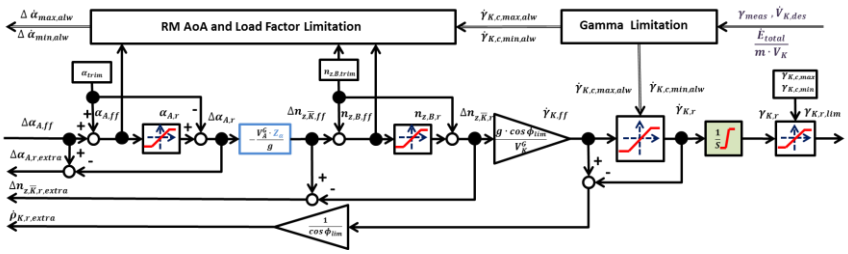

Fig. 7. Model of Load Factor and Flight Path Angle

4.2. Longitudinal Envelope Protections

Here following the speed protection case, the phase plane protection concept is used to form the protection signals as input for the dynamic limitation block. To save space, only the upper bound of the protected signal is shown here, as the lower bound is symmetric mirror of this structure. Most of the protection implementation is well illustrated by the figures nearby.

4.2.1. Flight Path Angle Limitation

Besides the absolute limit of the flight path angle, another limit from energy consideration is also introduced:
As is well known, the total energy of the aircraft could be described as

$$E_{total} = 1/2 \cdot mV_K^2 + mgh \tag{28}$$

The energy change rate is

$$\dot{E}_{total} = mV_K\dot{V}_K + mg\dot{h} = mV_K\dot{V}_K + mgV_K \cdot \sin\gamma_K \tag{29}$$

If the throttle is fixed, indicating no external energy is flowing into the system and the allowed speed change rate $\dot{V}_{K,alw}$ is specified, then the achievable flight path angle limited by this energy condition is:

$$\gamma_K = \arcsin((\dot{E}_{total}/mV_K - \dot{V}_{K,alw})/g) \tag{30}$$

Both the absolute and energy limits are considered as shown in figure 8.

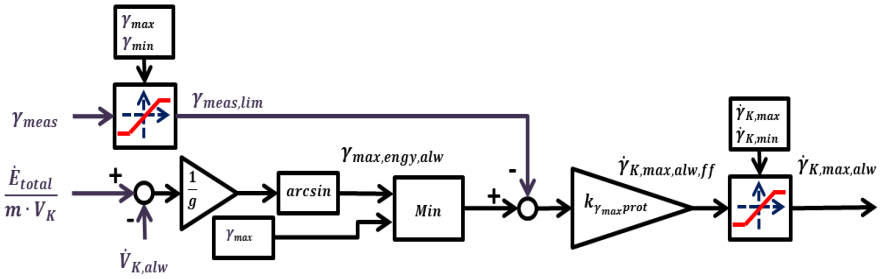

Fig. 8. Flight Path Angle Limitation

4.2.2. Reference Model AoA and Load Factor Limitation

The limitation of the both AoA and load factor can be done at the same time as both of them could be limited by limiting the rate change of AoA, which physically is the source of change in the AoA or load factor.

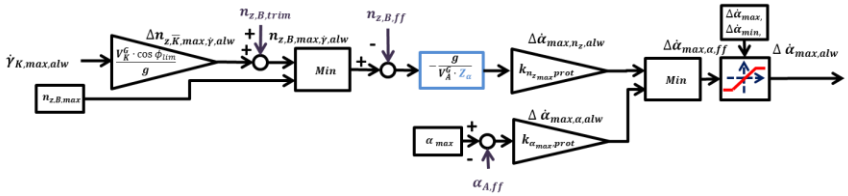

Fig. 9. Reference Model AoA and Load Factor Limitation

The saturation information from the flight path angle model is represented by the maximum allowed flight path angle rate $\dot{\gamma}_{K,\max,alw}$. In contrast to the command loop, in the protection loop, $\dot{\gamma}_{K,\max,alw}$ is converted back to the maximum allowable incremental of load factor $\Delta n_{z,\bar{K},\max,\dot{\gamma},alw}$. In the next step after adding the current trim part of the load factor, the maximum allowed load factor limited by flight path angle $n_{z,B,\max,\dot{\gamma},alw}$ could be obtained. Then the smaller one when compared to the absolute load factor upper bound due to structure stiffness, would be selected as the final upper bound of the allowable load factor.

Note that the limitation is only done within the reference model, that is with this structure, closed loop response of AoA, for instance, would not be expected to be still in the safe range, as the error dynamics induced by the controller would makes the transient close loop response be different from the reference command to be followed. Nevertheless, this limitation in the reference model is still necessary, as the tracking error of a successfully designed controller will converge to zero, then the closed loop AoA would follow the reference command in the steady state.

4.2.3. Pitch Angle Limitation

For pitch angle limitation, the pitch angle differential equation (7) is used to bound pitch rate,

$$q_{K_{\max},\theta,alw} = \left(\dot{\theta}_{\max,alw} + r_K \cdot \sin\phi\right) / \cos\phi \tag{31}$$

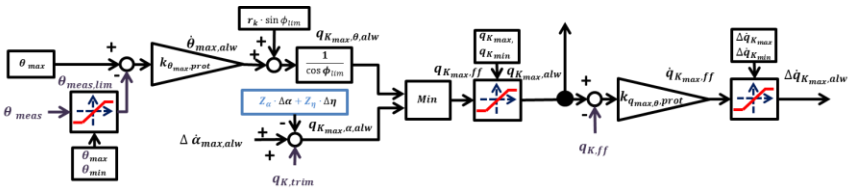

Fig. 10. Pitch Angle Limitation

Another factor from AoA and load factor limitation is considered dynamically by solving for the allowed pitch rate when the allowed rate change of AoA is limited. As shown in figure 10.

$$\Delta q_{K_{\max},\alpha,alw} = \Delta\dot{\alpha}_{\max,alw} - Z_\alpha \cdot \Delta\alpha - Z_\eta \cdot \Delta\eta \tag{32}$$

4.2.4. Actuator Limitation

There is one point to be mentioned for actuator limitation, the information from other protections are carried by $\Delta\dot{q}_{K_{\max},alw}$ and used here through the equation:

$$\Delta\eta_{\max,\Delta\dot{q},alw} = \left(\Delta\dot{q}_{K_{\max},alw} - M_{\alpha,des} \cdot \Delta\alpha - M_{q,des} \cdot \Delta q\right) \Big/ M_\eta \tag{33}$$

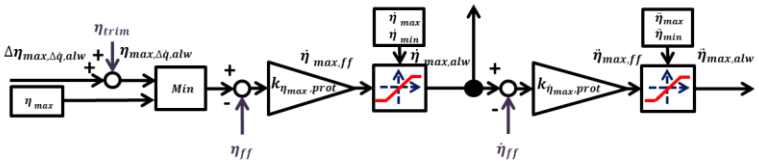

Fig. 11. Actuator Model with Limits

4.3. Lateral and Directional Reference Model Architecture

The general architecture for lateral and directional reference model is shown in figure 12

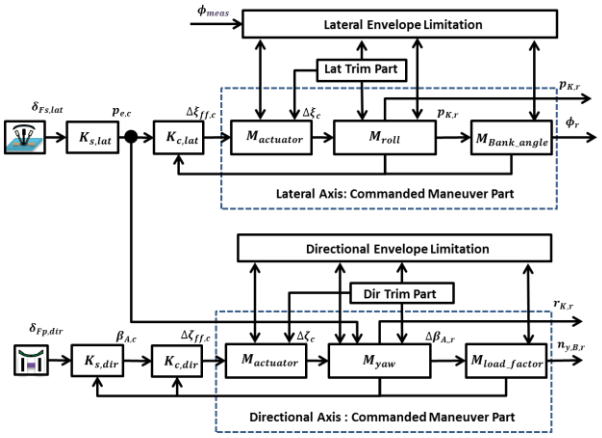

Fig. 12. Architecture of the Lateral and Directional Reference Model

4.3.1. Lateral Reference Model

For lateral reference model, roll channel dynamics featuring a first order behavior is implemented here.

$$\Delta\dot{p}_K = L_{p,des} \cdot \Delta p_K + L_\xi \Delta\xi \tag{34}$$

As lateral stick deflection is commanding velocity vector roll, the body fixed frame roll rate command is simply:

$$\Delta p_{K,c} = p_{e,c} \cdot \cos\alpha_A \tag{35}$$

Spiral stability can be restored for bank angle $48^\circ \prec |\phi| \le 75^\circ$ by actively adding proper roll rate to obtain the roll reference command as shown in figure 13. However, by this way, even with full lateral stick deflection, the maximum achieved bank angle can not reach exactly 75°. Moreover, to prevent stall due to turn compensation in large bank angles, trimmed AoA is also seen as a factor to limit the bank angle, as

$$\alpha_{trim} = C_L^{-1} \cdot \cos\theta \cdot mg / (\cos\phi \cdot \bar{q} \cdot S) \tag{36}$$

The lateral reference model structure is shown in figure 13.

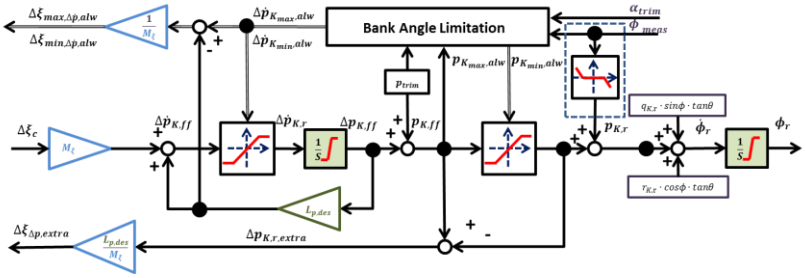

Fig. 13. Lateral Reference Model

4.3.2. Directional Reference Model and Envelope Protection

The directional reference model is specified as a second order system.

$$\begin{bmatrix} \Delta\dot{r}_K \\ \Delta\dot{\beta}_A \end{bmatrix} = \begin{bmatrix} N_{r,des} & N_{\beta,des} \\ -1 & Y_\beta \end{bmatrix} \begin{bmatrix} \Delta r_K \\ \Delta\beta_A \end{bmatrix} + \begin{bmatrix} N_\varsigma \\ Y_\varsigma \end{bmatrix} \Delta\varsigma \tag{37}$$

One special point is the fact that yaw rate also contributes to the evolution of pitch angle, and shall be limited to complete the pitch angle limitation. From the pitch angle differential equation (7)

$$r_{K_{\max},\theta,alw} = \left(q_K \cdot \cos\phi - \dot{\theta}_{\max,alw}\right) / \sin\phi \tag{38}$$

Since this equation would become singular at zero bank angle. Another strategy is used here, that is the yaw rate command $\Delta r_{K,ff}$, shall be limited as a function of current pitch angle.
With

$$\Delta r_{K,ff} = p_{e,c} \cdot \sin \alpha_A + \Delta r_{K,r} \tag{39}$$

The allowable $\Delta r_{K,ff}$ is implemented as shown in figure with the logic in the table 2.

Table 2. Allowable $\Delta r_{K,ff}$ When Pitch Angle Hits the Envelope Boundary

$\Delta r_{K,r}$	$\theta = 50^\circ$	$\theta = -50^\circ$
$\phi \geq 0$	$\left[0^\circ \sim 100^\circ \cdot K_{\theta_{\min},prot}\right]$	$\left[-100^\circ \cdot K_{\theta_{\max},prot} \sim 0^\circ\right]$
$\phi \prec 0$	$\left[-100^\circ \cdot K_{\theta_{\min},prot} \sim 0^\circ\right]$	$\left[0^\circ \sim 100^\circ \cdot K_{\theta_{\max},prot}\right]$

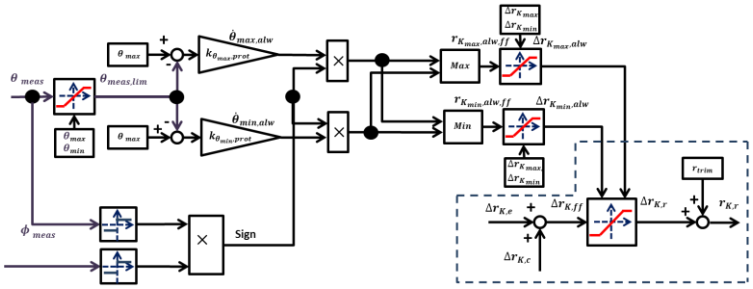

Fig. 14. Logic to Limit Yaw Rate for Pitch Angle Limitation

5. Simulation Results

The feasibility of this reference model is illustrated by trimming and linearizing a general aviation aircraft (Diamond DA42) model in straight and level flight at the speed of 93 knots and height of 1500 m, the attitude response of the reference model is restored using equation (6)-(8), with reference rotation rates.
Simulation results are shown in figure 15, the dashed or dotted lines are limits for the signals. For the stick deflection during the period $t = 2 \sim 4$ seconds, no limits are violated.

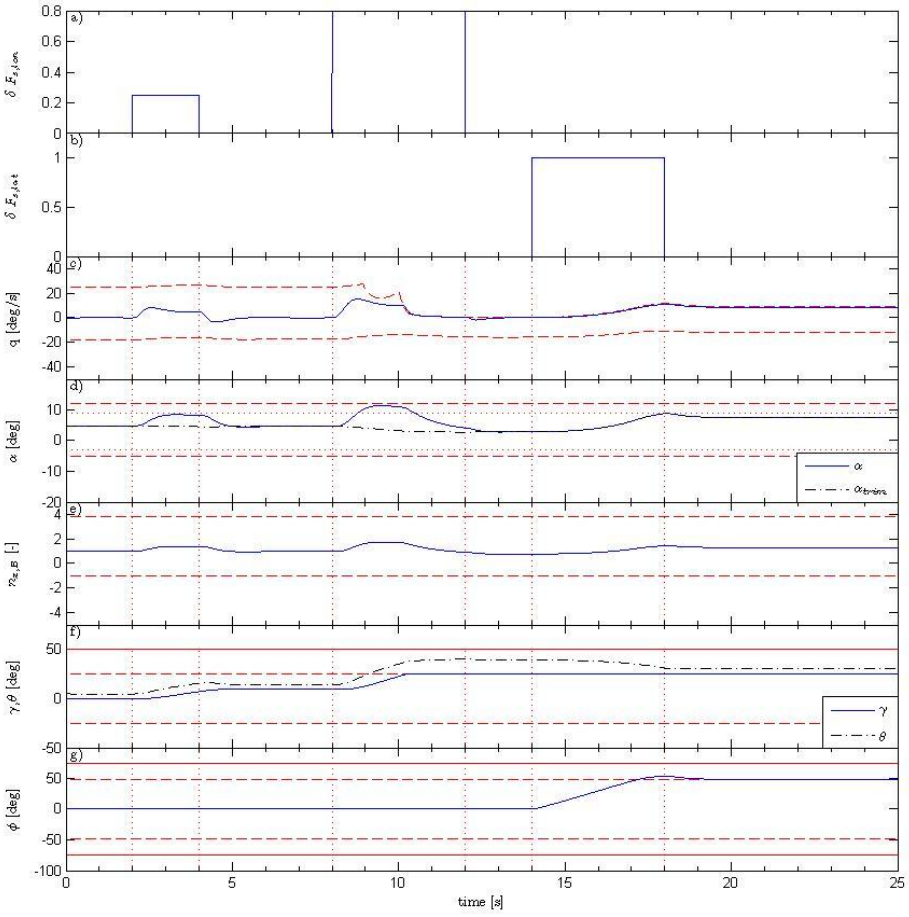

Fig. 15. Response of the Reference Model to the Stick Commands

A flight path rate command/flight path angle hold response could be seen in figure 15 (f), pitch rate (c) and AoA (d) response are typical aircraft response to a step command. Then a even larger pull is given by the stick from $t = 8 \sim 12$ seconds, the flight path angle soon reaches its limit at about $t = 10.2$ seconds, the limitation is evident to be effective as the nose of the reference aircraft starts to pitch down (figure 15 (c)), the reference pitch rate hits its upper bound and remains constrained by its upper bound as long as the flight path angle is at its upper bound, and the commanded AoA is automatically being reduced although the stick

still pulls for more flight path angle till $t = 12$, the trimmed AoA (figure 15 (d), dash-dot line) is getting smaller as not so much load factor is needed for a higher pitch angle (recall equation (5)), this is a physically meaningful consequence of the aircraft response to envelope protection.

During the period $t = 14 \sim 18$, and full lateral stick deflection is commanded, as time elapses, the bank angle starts to build, then turn compensation could be seen working as shown in figure 15 (d) and (e), more lift is being generated as bank angle is increasing, to leave 3° space for pilot's active maneuver command, the trimmed AoA is limited to $-2^\circ \le \alpha_{trim} \le 9^\circ$, further deflection of lateral stick would be neglected if α_{trim} reaches its upper bound. A velocity vector roll could be partly seen as pitch angle started to go down to help for the rolling around velocity vector during this period. The spiral stability is restored as the bank angle returns to 48° degree at the release of the stick. Another functionality, turn coordination could also be seen after $t = 18$, because the reference aircraft dynamics is holding both pitch angle and bank angle unchanged.

During all the simulation time, the AoA, load factor and pitch angle are well within the envelope defined by the functionality requirements in table 1.

6. Conclusion

The usefulness of the proposed reference model architecture is demonstrated by numerical simulation, as the results shown it could fulfill the functionality requirements. A more intuitive way to evaluate the reference model is to fly manually with joystick and visualize with software like Flight Gear, this part is omitted here.

To conclude, this reference model architecture has two benefits. Firstly, a unique reference model taking into account flight dynamics, actuator dynamics and limits and envelope protection aspects. The designer could understand immediately the consequence of modifying the reference model, as it seems to be a copy of the aircraft and all the signals have their physical meaning, previous knowledge of flight dynamics applies to the reference model. Secondly, the non-cascaded structure decoupled the specific controller design with the desired reference dynamics, whereas the reference dynamics could be seen as the ideal dynamics formed by requirements. Hence at an early age of flight control system design, the ideal dynamics including envelope protections could already be evaluated by piloted simulation, and thus reduces the iteration in the design cycle.

More aspects concerning this nonlinear reference model could be explored in the future such as design the parameters in a way to provide good flying qualities. Another interesting aspect could be increasing pilot's awareness of protection situation by audio warning or stick force change.

7. Acknowledgement

Special thanks must be given to Dipl.-Ing. Falko Shuck for providing the model of the general aviation aircraft. The authors also thank the reviewers for the helping comments.

Reference

1. Lambregts, A. A., and Cannon, D. G. : Development of a Control Wheel Steering Mode and Suitable Displays that Reduce Pilot Workload and Improve Efficiency and Safety of Operation in the Terminal Area and in Windshear, Proceedings of the AIAA Guidance, Navigation, and Control Conference, AIAA, New York, pp. 609–620(1979)
2. M.M.K.V. Sankrithi, W.F. Bryant.:7J7 Manual Flight Control Functions. AIAA paper 87-2454(1987).
3. E. C. Stewart, W. A. Ragsdale, A. J. Wunschel.: An Evaluation of Automatic Control System Concepts for General Aviation Airplanes. AIAA Atmospheric Flight Mechanics Conference, Minneapolis, MN; United States; pp. 330-343, 15-17 Aug. (1988).
4. Van der Geest, P., Nieuwpoort, A., and Borger, J.: A Simulator Evaluation of Various Manual Control Concepts for Fly-by-Wire Transport Aircraft, Proceedings of the AIAA Guidance, Navigation, and Control Conference, AIAA, Washington, DC, pp. 181–199 (1992).
5. M. Mulder,A. R. Veldhuijzen, M. M. van Paassen, J. A. Mulder.: Integrating Fly-by-Wire Controls with Perspective Flight-Path Displays. Journal of guidance, control and dynamics.Vol. 28, No. 6(November–December 2005).
6. C. Borst, M. Mulder, M. M. van Paassen, and J. A. Mulder.: Path-Oriented Control/Display Augmentation for Perspective Flight-Path Displays. Journal of Guidance, Control, and Dynamics. Vol. 29, No. 4, July–August(2006)
7. F. Holzapfel, F. Schuck, L. Höcht, G. Sachs. Flight Dynamics Aspects of Path Control. AIAA Guidance, Navigation and Control Conference and Exhibit, Hilton Head, South Carolina. 20 - 23 August (2007).
8. Holzapfel F., Sachs G.: Dynamic Inversion Based Control Concept with Application to an Unmanned Aerial Vehicle. AIAA Guidance, Navigation and Control Conference and Exhibit: AIAA-2004-4907 (2004)
9. Johnson E. Limited Authority Adaptive Flight Control, PhD thesis, Georgia Institute of Technology (2000).
10. B.L. Stevens and F.L. Lewis.: Aircraft Control and Simulation, John Wiley and Sons Inc (2003).
11. Tischler, M. B.: Advances in Aircraft Flight Control, Taylor & Francis (1996)
12. Gibson, J.: The Definition, Understanding and Design of Aircraft Handling Qualities, Delft University Press. (1997).
13. Gibson J. Development of a design methodology for handling qualities excellence in fly by wire aircraft (1999).
14. Anon. Flying Qualities of Piloted Aircraft MIL-HDBK-1797. US Department of Defense (1997).
15. Flight Control Design-Best Practices. AGARD Report, RTO-TR-029. (December 2000).
16. Wünnenberg H. Handling Qualities of Unstable Highly Augmented Aircraft. AGARD Advisory Report.29–29(1991).
17. Diamond Aircraft. Airplane Flight Manual DA-42 NG(2009)